Theor Chim Acta (1991) 80: 223–243

Theoretica Chimica Acta

Method of moments approach and coupled cluster theory

Karol Jankowski[1,2], **Josef Paldus**[1,3,*], **and Piotr Piecuch**[1,**]

[1] Department of Applied Mathematics, University of Waterloo, Waterloo, Ontario, Canada N2L 3G1

[2] Quantum Chemistry Group, Institute of Physics, Nicholas Copernicus University, ul. Grudziadzka 5, 87-100 Toruń, Poland

[3] Department of Chemistry and Guelph-Waterloo Center for Graduate Work in Chemistry, Waterloo Campus, University of Waterloo, Waterloo, Ontario, Canada N2L 3G1

Received November 22, 1989; received in revised form November 29, 1990/Accepted February 1, 1991

Summary. The single reference coupled cluster (CC) approach to the many-electron correlation problem is examined from the viewpoint of the method of moments (MM). This yields generally an inconsistent (overcomplete) set of equations for cluster amplitudes, which can be solved either in the least squares sense or by selective projection process restricting the number of equations to that of the unknowns. These resulting generalized MM–CC equations always contain the standard CC equations as a special case. Since, in the MM–CC formalism, the Schrödinger equation will be approximately satisfied on a subspace spanned by non-canonical configurations, this procedure may be helpful in extending the standard single reference CC theory to quasi-degenerate situations. To examine the potential usefulness of this idea, we explore the linear version of the CC approach for systems with a quasi-degenerate reference, in which case the standard linear theory is plagued with singularities due to the intruder states. Implications of this analysis for the structure of the wavefunction are also briefly discussed.

Key words: Coupled cluster approach – Method of moments approach – Many-electron correlation problem – Intruder states – Quasi-degeneracy

1. Introduction

This decade witnesses a remarkable development in coupled cluster (CC) methods for an accurate and reliable determination of many-electron correlation effects in atoms and molecules (for recent overviews and developments, see, e.g., [1–6]). Although substantial headway is being made in the important area of formulating open-shell CC techniques (see, e.g., [4, 6, 7]), even more significant progress has been achieved in computational implementations of single reference

---

[*] Killam Research Fellow 1987–89

[**] *Permanent address*: Institute of Chemistry, University of Wrocław, F. Joliot-Curie 14, 50-383 Wrocław, Poland

CC methods [4, 8–14]. The latter, together with an enormous increase in the power of today's computers, are shaping into a standard quantum chemical procedure capable of providing highly accurate molecular data for numerous medium sized systems of practical interest. However, the majority of these applications are only concerned with the energy of the systems involved, while relatively little attention is paid to the corresponding CC wavefunctions.

The aim of this paper is to analyze the closed-shell CC formalism from the viewpoint of the method of moments (MM), (cf., e.g., [15]), as applied to the solutions of the electronic Schrödinger equation [16–18]. This approach will enable us to shed new light on certain aspects of CC methods as well as to design modifications that avoid singular behavior of CC equations in quasi-degenerate situations, particularly singularities that plague the linear CC (L–CC) approach [19–21]. We shall also pay attention to the structure of the CC wavefunction and its uniqueness from the viewpoint of the MM.

2. Essentials of the single reference CC approach

From the time of pioneering work by Coster and Kümmel [22] and Čížek [23], numerous derivations and discussions of the CC approach were put forward by various authors (for overview, see, e.g., [1–4]). We thus recall here only a few essential points that are relevant to our study.

2.1. Exact solutions

Let us consider the N-electron Schrödinger equation:

$$(H - E)|\Psi\rangle = 0, \tag{1}$$

where $|\Psi\rangle$ designates the exact (non-degenerate) eigenstate that is associated with the ground state eigenvalue E. Consider, next, a set of spin orbitals $\{\phi_i\}$, containing a subset that defines a single-determinantal reference wavefunction $|\Phi\rangle$ that approximates $|\Psi\rangle$. The spin orbitals occupied in $|\Phi\rangle$ are labeled by $a, b, c, \ldots,$ the unoccupied ones by $r, s, t, \ldots,$ and the generic ones by $i, j, k, \ldots$. If the set $\{\phi_i\}$ is complete and appropriate convergence conditions are satisfied (cf., e.g., [24]), $|\Psi\rangle$ can be formally represented (using the intermediate normalization $\langle\Phi|\Psi\rangle = 1$) in the CI form as

$$|\Psi\rangle = (1 + \hat{C})|\Phi\rangle, \tag{2}$$

with

$$\hat{C} = \sum_{n=1}^{N} C_n, \tag{3}$$

where the n-body excitation operator C_n is given, in the second quantized form, as follows

$$C_n = (n!)^{-2} \sum_{\substack{a_1 \cdots a_n \\ r_1 \cdots r_n}} c^{r_1 r_2 \cdots r_n}_{a_1 a_2 \cdots a_n} e^{r_1 r_2 \cdots r_n}_{a_1 a_2 \cdots a_n}, \tag{4}$$

with

$$e^{r_1 r_2 \cdots r_n}_{a_1 a_2 \cdots a_n} = X^\dagger_{r_1} X^\dagger_{r_2} \cdots X^\dagger_{r_n} X_{a_n} \cdots X_{a_2} X_{a_1}. \tag{5}$$

Since for realistic N-electron systems the c-coefficients in the expansion (4) are not available, one resorts to a molecular orbital (MO) description and considers a component of $|\Psi\rangle$ in a finite dimensional N-electron space, built as an antisymmetrized tensor power of a (finite) spin orbital set $\{\phi_i\}$. Then all the summations in the expansion (4) are finite and the CI coefficients c can be determined (at least in principle) by applying Rayleigh–Ritz variational method. The resulting full CI (FCI) wavefunction, which we again designate by $|\Psi\rangle$, represents then an exact solution within the chosen finite dimensional model space, which is defined by a chosen spin orbital set $\{\phi_i\}$. These "exact" solutions can serve as a useful benchmark for testing of various approximate theories within the same model space. For the purposes of the present analysis there is no need to differentiate between the exact (i.e., truly converged) and "exact" FCI wavefunctions.

In the many-body perturbation theory (MBPT) [25] formalism, a nondegenerate N-electron wavefunction $|\Psi\rangle$ is given in each order of PT by the sum of all possible *linked* diagrams, including the exclusion principle violating (EPV) diagrams. It was first shown by Hubbard [26] that such a wavefunction can be uniquely expressed in terms of *connected* diagrams of the MBPT. Designating by $\hat{T}$ the operator that generates this set of connected diagrams, when acting on a chosen independent particle model reference state $|\Phi\rangle$, the exact wavefunction $|\Psi\rangle$ is then expressed as follows:

$$|\Psi\rangle = \exp(\hat{T})\,|\Phi\rangle. \tag{6}$$

This expansion is nowadays referred to as a cluster expansion due to its similarity with an analogous expansion that is exploited in statistical mechanics (see, e.g., [27]). The operator $\hat{T}$, Eq. (6), is correspondingly referred to as a cluster (expansion) operator. It consists of various n-particle components T_n,

$$\hat{T} = \sum_{n=1}^{N} T_n, \tag{7}$$

which in the second quantization formalism are defined through the corresponding cluster amplitudes t,

$$T_n = (n!)^{-2} \sum_{\substack{a_1 \cdots a_n \\ r_1 \cdots r_n}} t^{r_1 r_2 \cdots r_n}_{a_1 a_2 \cdots a_n} e^{r_1 r_2 \cdots r_n}_{a_1 a_2 \cdots a_n}. \tag{8}$$

These amplitudes are simply related with the corresponding c-amplitudes of the FCI expansion, namely [22, 23, 28]:

$$\begin{aligned} C_1 &= T_1, \\ C_2 &= T_2 + \tfrac{1}{2}T_1^2, \\ C_3 &= T_3 + T_1T_2 + \tfrac{1}{6}T_1^3, \\ C_4 &= T_4 + \tfrac{1}{2}T_2^2 + \tfrac{1}{2}T_1^2T_2 + T_1T_3 + \tfrac{1}{24}T_1^4. \end{aligned} \tag{9}$$

These equations can always be solved for T_n. Hence, the knowledge of the CI structure of the exact wavefunction uniquely determines its structure in terms of the exponential of the cluster operator, i.e., the CI form, Eq. (2), is equivalent to the CC form, Eq. (6).

2.2. Approximate solutions

An application of either the CI or CC method to actual many-electron systems requires invariably an imposition of drastic restrictions on the order of excitation operators that are retained in Eqs. (3) or (7), respectively. Thus, generally, we assume that

$$\hat{C} \approx \sum_{n=1}^{n_{\mathrm{CI}}} C_n, \tag{10a}$$

and

$$\hat{T} \approx T = \sum_{n=1}^{n_{\mathrm{CC}}} T_n, \tag{10b}$$

with

$$n_{\mathrm{CI}} < N \quad \text{and} \quad n_{\mathrm{CC}} < N. \tag{10c}$$

In the following we designate the truncated cluster operator by T. For the most often used CISD and CCSD approaches, we have $n_{\mathrm{CI}} = n_{\mathrm{CC}} = 2$.

The c-amplitudes of the limited CI approaches are obtained from the standard variational Rayleigh–Ritz procedure. The resulting secular equation for $|\Psi_{\mathrm{CI}}\rangle$ and the approximate energy E_{CI} may be written in the form:

$$\langle \Phi | H - E_{\mathrm{CI}} | \Psi_{\mathrm{CI}} \rangle = 0, \tag{11a}$$

$$\left\langle \begin{matrix} r_1 \cdots r_n \\ a_1 \cdots a_n \end{matrix} \middle| H - E_{\mathrm{CI}} \middle| \Psi_{\mathrm{CI}} \right\rangle = 0, \qquad (n = 1, 2, \ldots, n_{\mathrm{CI}}), \tag{11b}$$

where the excited configurations are denoted as

$$\left| \begin{matrix} r_1 \cdots r_n \\ a_1 \cdots a_n \end{matrix} \right\rangle = e^{r_1 \cdots r_n}_{a_1 \cdots a_n} |\Phi\rangle, \tag{12}$$

and all the configurations appearing in the C_n operators of Eq. (10a) are accounted for.

Formally, Eqs. (11a) and (11b) can be obtained as projections of the Schrödinger Eq. (1) onto the *projection space* spanned by the reference configuration $|\Phi\rangle$ and by all the excited configurations appearing in the expansion of $|\Psi_{\mathrm{CI}}\rangle$. Thus, the CI equations may be regarded as a special case of the MM method [15–18], or of its linear realization known as Galerkin–Petrov method [18, 29]. Using the terminology of this latter approach [18], the CI equations result when the *coordinate space* (used to approximate the eigenfunctions) and the *projection space* (onto which the Schrödinger Eq. (1) is projected) are identical.

In contrast to CI methods, the t-amplitudes of CC approaches (and the corresponding energy) cannot be easily obtained by exploiting a standard variational procedure. Indeed, exploitation of the CC ansatz, Eq. (6), in the variational functional leads to an infinite expansion involving arbitrarily high powers of t-amplitudes, even when truncated expansion is used for the cluster operator, Eq. (10b). Consequently, CC approaches are based on nonvariational procedures. The explicit equations for the t-amplitudes were first derived by Čížek [23] using the MBPT diagrammatic techniques. However, it was subsequently shown [30] that the same equations can be obtained when using standard configurational (first quantization) methods based on projecting the Schrödinger equation, i.e. by the MM procedures. Since that time the explicit projection-type derivation of the CC equations was often employed. Using this approach, one can employ either of the following two methods. The first one [30] projects the Schrödinger equation

$$(H - E_{\mathrm{CC}})|e^{T}\Phi\rangle = 0 \tag{13}$$

onto the $|\Phi\rangle$ and the set of excited configurations. This set is always chosen to contain those configurations which are used to represent the operators T_n appearing in Eq. (10b). The resulting equations can be written in the following implicit form:

$$\langle\Phi|H - E_{\mathrm{CC}}|e^{T}\Phi\rangle = 0, \tag{14a}$$

$$\left\langle \begin{matrix} r_1 \cdots r_n \\ a_1 \cdots a_n \end{matrix} \middle| H - E_{\mathrm{CC}} \middle| e^{T}\Phi \right\rangle = 0, \qquad (n = 1, 2, \ldots, n_{\mathrm{CC}}). \tag{14b}$$

For example, in the CCSD approach, where $T = T_1 + T_2$ and $n_{\mathrm{CC}} = 2$, the equations corresponding to projections onto the singly- and doubly-excited configurations are accounted for.

The second method takes advantage of a simple transformation proposed by Coester [22], which leads from the Schrödinger equation for $|\Psi\rangle$, expressed in the CC form of Eq. (6), to the equation

$$(e^{-T}He^{T} - E_{\mathrm{CC}})|\Phi\rangle = 0. \tag{15}$$

This equation is projected onto $|\Phi\rangle$ and the same set of excited configurations as in the previous case, obtaining now the following set of implicit equations:

$$\langle\Phi|e^{-T}He^{T}|\Phi\rangle = E_{\mathrm{CC}}, \tag{16a}$$

$$\left\langle \begin{matrix} r_1 \cdots r_n \\ a_1 \cdots a_n \end{matrix} \middle| e^{-T}He^{T} \middle| \Phi \right\rangle = 0, \qquad (n = 1, 2, \ldots, n_{\mathrm{CC}}) \tag{16b}$$

or, equivalently,

$$\langle\Phi|(He^{T})_C|\Phi\rangle = E_{\mathrm{CC}}, \tag{16a$'$}$$

$$\left\langle \begin{matrix} r_1 \cdots r_n \\ a_1 \cdots a_n \end{matrix} \middle| (He^{T})_C \middle| \Phi \right\rangle = 0, \qquad (n = 1, 2, \ldots, n_{\mathrm{CC}}), \tag{16b$'$}$$

where the subscript C indicates the connected component of a given expression. The latter two equations are an immediate consequence of the identity [23]

$$H|e^{T}\Phi\rangle = (He^{T})_C|e^{T}\Phi\rangle = e^{T}(He^{T})_C|\Phi\rangle. \tag{13$'$}$$

In contrast to Eqs. (14b), Eqs. (16b) or (16b′) are manifestly connected, thus immediately implying the size extensivity [28, 31] of an approximate CC approach considered. It should be noted that the energy is now removed from Eqs. (16b) that determine t-amplitudes. Of course, Eqs. (14b) are also energy independent when their explicit form is worked out [30], since the disconnected component is exactly cancelled by the energy dependent term. Indeed, both Eqs. (14b) and (16b) represent equivalent sets of non-linear equations that determine the CC amplitudes and thus the energy.

For the exact T operator ($n_{\mathrm{CC}} = N$) the proof of the equivalence of Eqs. (14a,b) and (16a,b) is straightforward (see, e.g., [32]). For approximate T operators ($n_{\mathrm{CC}} < N$), the equivalence can be proved by properly combining the equations for different n values. An explicit proof of this equivalence was recently given for the CCSD method [33].

3. Method of moments aspects of the CC method

In the preceding section we presented standard versions of CI and CC approaches as special cases of the method of moments. Although the projection technique that we used to obtain CI Eqs. (11a,b) and CC Eqs. (14a,b) or (16a,b) is the same, there is nevertheless a clear distinction between these two cases when regarded from the MM viewpoint. Namely, in the variational CI approach, the projection space is uniquely defined by the form of $|\Psi_{\mathrm{CI}}\rangle$, i.e., this space is given by the span of all determinants (or corresponding spin-adapted configurations) that appear in $|\Psi_{\mathrm{CI}}\rangle$ (coordinate space of MM). This is a direct consequence of applying the variational principle to determine $|\Psi_{\mathrm{CI}}\rangle$. However, in nonvariational CC methods, there is no obvious *a priori* principle that fixes the projection space, leaving thus certain freedom to select this space arbitrarily (cf., however, [34]). This freedom was seldom discussed in the literature and all the applications exploit the same projection space as in the corresponding CI procedure. The main argument to motivate this choice is of a practical nature, since it enables one to obtain a correct number of equations for the unknown t-amplitudes (see, e.g., [3, 33]). Another argument is based on the observation [30] that CC Eqs. (14b) may be derived from CI Eqs. (11b) by approximating c-amplitudes representing higher excitations by products of t-amplitudes associated with corresponding excitations of lower order. Perhaps the most convincing argument for the use of a standard projection space is the fact that the equations so obtained enable a straightforward interpretation of t-amplitudes in terms of the MBPT (see, e.g., [35]). We will not address this problem here but instead will discuss the structure of the CC equations for other than standard choices of the projection space.

3.1. *Alternative choices of projection spaces*

From a purely mathematical viewpoint, there are many possibilities how to choose projection spaces that can be used to derive equations determining CC amplitudes. We shall limit our considerations to spaces that are spanned by the N-electron configurations constructed from the same one-electron spin orbitals that are used to define the N-electron coordinate space, i.e., $|\Phi\rangle$ and the operator T. These spaces represent subspaces of the N-electron component of the Fock space $\mathscr{F}_N$ generated by $|\Phi\rangle$ and all single, double, etc., up to N-tuple excitations:

$$\mathscr{F}_N = \mathrm{Span}\left\{|\Phi\rangle, \left|\begin{matrix} r_1 \\ a_1 \end{matrix}\right\rangle, \left|\begin{matrix} r_1 r_2 \\ a_1 a_2 \end{matrix}\right\rangle, \ldots, \left|\begin{matrix} r_1 \cdots r_N \\ a_1 \cdots a_N \end{matrix}\right\rangle\right\}, \tag{17}$$

with a_j and r_j ranging over the occupied and unoccupied spin orbitals, respectively.

In standard CC approaches, Eqs. (13) or (15) are projected onto a subset of the spanning set in Eq. (17) consisting of $|\Phi\rangle$ and of all the excited configurations that result from $|\Phi\rangle$ by action of the excitation operators appearing in the approximate cluster operator T considered. However, as already alluded to above, we can also choose to project onto configurations from Eq. (17) that do not belong to a standard set. We shall refer to such projections as *nonstandard* ones. Since our Hamiltonian H contains at most two-electron operators, it is easily seen that projections of Eq. (15) onto highly excited configurations will trivially vanish, which will make them useless from the MM viewpoint. Moreover, nonstandard projections of Eq. (13) may produce linear combination of equations that are associated with projections on configurations of lower excitation order. (Note that unlike the equations that are associated with standard projections, the nonstandard projections of Eqs. (13) and (15) may lead to nonequivalent sets of equations.) Even though projections on some members of the spanning set (17) are trivially satisfied, the number of equations that result by nonstandard projections is usually much larger than the number of t-amplitudes to be determined.

In view of these facts, the questions of the interpretation and of the possible usefulness of nonstandard equations in many-electron theory arise. Let us briefly address the latter one. Clearly, exploiting the additional (nonstandard) equations together with the standard ones will result in an inconsistent (or overcomplete, or overdetermined) system of equations. However, these equations can be satisfied in the least squares sense (by minimizing the sum of squares of their left-hand sides). Since these equations are not linear, this may not be an easy task. However, one could at least consider approximate modifications of the standard t-amplitudes when imposing the MM requirements or examine how accurately are these nonstandard equations satisfied by standard CC amplitudes.

One could also use the nonstandard equations to replace some of the standard ones, keeping the number of equations to be equal to that of the unknown cluster amplitudes. This replacement, or selective projection, could be done in such a way so as to remove those standard equations which involve cluster components associated with intruder states and are responsible for the singular behavior of the corresponding linear approximation. However, it is not *a priori* clear how such replacements should be carried out, so that any such scheme will be more or less arbitrary. From this viewpoint, the least squares approach is certainly to be preferred (cf., however, Sect. 4). In order to simplify further discussion, we restrict ourselves in the following to the CPMET [23] (or CCD) equations, which may be regarded as representing a fundamental CC approach.

3.2. Method of moments approach to CCD

Let us first consider projections of Eq. (15) with $T = T_2$ onto all the excited configurations belonging to the spanning set for $\mathscr{F}_N$, Eq. (17). Since H involves at most two-electron operators, projections onto higher than sixtuply-excited configurations will identically vanish, leaving the following inconsistent system of implicit equations for the t_2-amplitudes:

$$\langle (1) | H_N | (1 + T_2)\Phi \rangle_C = 0, \tag{18a}$$

$$\langle (2) | f_N | T_2 \Phi \rangle_C + \langle (2) | V_N | (1 + T_2 + \tfrac{1}{2} T_2^2)\Phi \rangle_C = 0, \tag{18b}$$

$$\langle (3) | f_N | \tfrac{1}{2} T_2^2 \Phi \rangle_C + \langle (3) | V_N | (T_2 + \tfrac{1}{2} T_2^2)\Phi \rangle_C = 0, \tag{18c}$$

$$\langle (4) | V_N | (\tfrac{1}{2} T_2^2 + \tfrac{1}{6} T_2^3)\Phi \rangle_C = 0, \tag{18d}$$

$$\langle (5) | V_N | \tfrac{1}{6} T_2^3 \Phi \rangle_C = 0, \tag{18e}$$

$$\langle (6) | V_N | \tfrac{1}{24} T_2^4 \Phi \rangle_C = 0, \tag{18f}$$

where $\langle (n)|$ is a shorthand notation for $\left\langle \begin{matrix} r_1 \cdots r_n \\ a_1 \cdots a_n \end{matrix} \right|$ and the subscript N denotes the normal form of operators [36]. As usual, f_N and V_N designate, respectively, the one- and two-body parts of the Hamiltonian H_N and [cf. Eq. (13′)] the subscript C indicates that only connected terms are to be retained. We shall refer to this system as the MM–CCD equations. If Hartree–Fock (HF) orbitals are used, i.e., if the Brillouin theorem (BT) holds, the projections onto mono- and tri-excited configurations simplify to

$$\langle (1)|V_N|T_2\Phi\rangle_C = 0, \tag{19a}$$

$$\langle (3)|V_N|(T_2 + \tfrac{1}{2}T_2^2)\Phi\rangle_C = 0. \tag{19b}$$

Notice that Eqs. (18b) represent standard CCD or CPMET equations. One could also consider Eqs. (18a) and (18b) as characterizing so-called BD (Brueckner-doubles) theory [37], (cf. also [38]), since Eq. (18a) can be satisfied by an appropriate orbital transformation, thus determining approximate Brueckner (maximum overlap) orbitals. However, we work here with a *fixed* chosen orbital set $\{\phi_i\}$ (usually the HF orbitals), so that Eq. (18a), together with Eqs. (18c–f) will typify the MM approach rather than represent the conditions for Brueckner orbitals.

Hugenholtz-like diagrams characterizing these equations when the HF orbitals are used are shown in Fig. 1. To get a better feeling for the significance of nonstandard equations, and thus at least partially answer the question raised earlier, we present in Table 1 the lowest order of perturbation theory in which the diagrams characterizing the individual terms of the left-hand side of Eqs. (18a–f) (for the general reference state) and (19a,b) (if the BT holds) would contribute to the correlation energy. This gives us a certain measure of the importance of various terms involved. We see from this table that this order increases with the excitation order of configurations onto which we project. The standard CPMET equations involve the terms of the second, third and the fourth order. Projections onto mono-excited configurations contain (for the general reference state) terms of the second and the third order, which indicates that their addition to the standard set of CPMET equations may have a strong effect on the t_2-amplitudes. For HF orbitals, however, the projections onto the mono- and triply-excited configurations involve the fourth order term. Thus, a consideration of these equations could modify the t_2-amplitudes to the same degree as the inclusion of non-linear terms in the CCD equations, which first contribute in the same order of PT. Equations corresponding to projections onto tetra-, penta- and hexa-excited configurations, Eqs. (18d–f), involve the terms of higher order than those appearing in standard equations and their effect on the t_2-amplitudes is likely to be negligible. We will thus ignore these equations and concentrate on Eqs. (18a–c) or (19a,b) only.

Consider, next, the projections of Eq. (13) with $T = T_2$ onto the configurations spanning $\mathscr{F}_N$, Eq. (17). Realizing that

$$(H_N - \Delta E_{\mathrm{CCD}})|e^{T_2}\Phi\rangle = e^{T_2}(e^{-T_2}H_N e^{T_2} - \Delta E_{\mathrm{CCD}})|\Phi\rangle,$$

where $\Delta E_{\mathrm{CCD}} = E_{\mathrm{CCD}} - \langle\Phi|H|\Phi\rangle$ is the CCD energy relative to the mean value $\langle\Phi|H|\Phi\rangle$ (e.g., the CCD correlation energy, when the HF orbitals are used), we can express the projection onto an arbitrary configuration $\langle (n)|$ as follows:

$$\langle (n)|(H_N - \Delta E_{\mathrm{CCD}})|e^{T_2}\Phi\rangle = \langle e^{T_2^\dagger}(n)|e^{-T_2}H_N e^{T_2} - \Delta E_{\mathrm{CCD}}|\Phi\rangle = 0, \tag{20}$$

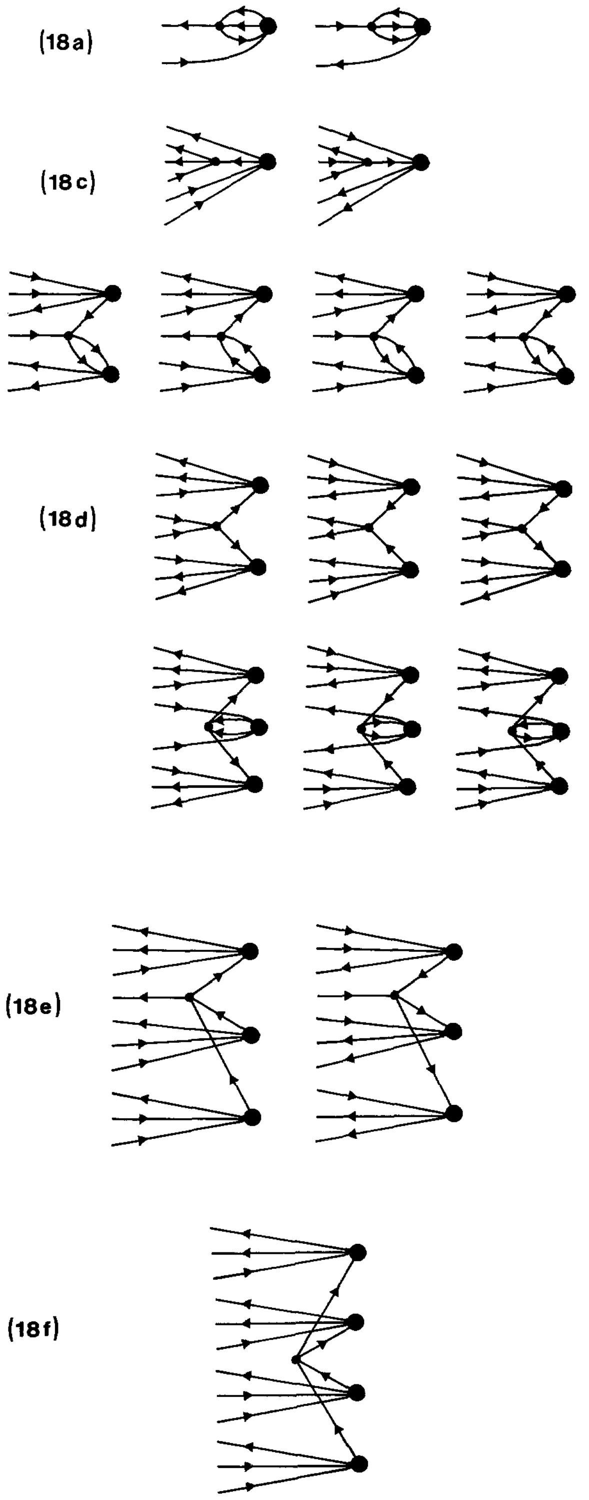

Fig. 1. Hugenholtz diagrams appearing in the nonstandard CCD equations when the HF orbitals are used. The numbers in parentheses refer to the corresponding equations in the text. Large and small full vertices represent t_2-amplitudes and antisymmetric two-electron integrals, respectively

Table 1. Lowest order of perturbation theory in which the diagrams (cf. Fig. 1 for the HF case) characterizing various terms of the nonstandard projections for the CCD approach can contribute to the correlation energy

Bra-states defining the equations (excitation order)	Term	Lowest order of PT	
		General reference	HF reference
$\langle(1)|$	1	2	—
	T_2	3	4
$\langle(2)|$	1	2	2
	T_2	3	3
	$\frac{1}{2}T_2^2$	4	4
$\langle(3)|$	T_2	4	4
	$\frac{1}{2}T_2^2$	5	5
$\langle(4)|$	$\frac{1}{2}T_2^2$	5	5
	$\frac{1}{6}T_2^3$	6	6
$\langle(5)|$	$\frac{1}{6}T_2^3$	7	7
$\langle(6)|$	$\frac{1}{24}T_2^4$	8	8

so that the projections of Eq. (13) can be expressed in terms of projections of Eq. (15) considered above. Exploiting this fact, we can write the projections of Eq. (13) in the following form:

$$\langle(1)|H_N|e^{T_2}\Phi\rangle_C = 0, \tag{21a}$$

$$\langle(2)|H_N|e^{T_2}\Phi\rangle_C = 0, \tag{21b}$$

$$\langle(3)|H_N|e^{T_2}\Phi\rangle_C + \tfrac{1}{4}\sum_{\substack{a,b\\r,s}} t_{ab}^{rs}\langle e_{rs}^{ab}(3)|H_N|e^{T_2}\Phi\rangle_C = 0, \tag{21c}$$

$$\langle(4)|H_N|e^{T_2}\Phi\rangle_C + \tfrac{1}{4}\sum_{\substack{a,b\\r,s}} t_{ab}^{rs}\langle e_{rs}^{ab}(4)|H_N|e^{T_2}\Phi\rangle_C = 0, \tag{21d}$$

$$\begin{aligned}\langle(5)|H_N|e^{T_2}\Phi\rangle_C &+ \tfrac{1}{4}\sum_{\substack{a,b\\r,s}} t_{ab}^{rs}\langle e_{rs}^{ab}(5)|H_N|e^{T_2}\Phi\rangle_C\\ &+ \tfrac{1}{32}\sum_{\substack{a,b\\r,s}}\sum_{\substack{c,d\\t,u}} t_{ab}^{rs}t_{cd}^{tu}\langle e_{rstu}^{abcd}(5)|H_N|e^{T_2}\Phi\rangle_C = 0,\end{aligned} \tag{21e}$$

$$\begin{aligned}\langle(6)|H_N|e^{T_2}\Phi\rangle_C &+ \tfrac{1}{4}\sum_{\substack{a,b\\r,s}} t_{ab}^{rs}\langle e_{rs}^{ab}(6)|H_N|e^{T_2}\Phi\rangle_C\\ &+ \tfrac{1}{32}\sum_{\substack{a,b\\r,s}}\sum_{\substack{c,d\\t,u}} t_{ab}^{rs}t_{cd}^{tu}\langle e_{rstu}^{abcd}(6)|H_N|e^{T_2}\Phi\rangle_C = 0,\end{aligned} \tag{21f}$$

where $e_{r_1\cdots r_n}^{a_1\cdots a_n} = (e_{a_1\cdots a_n}^{r_1\cdots r_n})^\dagger$. Since $\langle e_{rs}^{ab}(n)| \in \mathrm{Span}\{\langle(n-2)|\}$ and $\langle e_{rstu}^{abcd}(n)| \in \mathrm{Span}\{\langle(n-4)|\}$, the sums in Eqs. (21c–f) represent linear combinations of left-hand sides of projections on lower-excited configurations, e.g., the sums in Eqs. (21c) and (21d) contain the left-hand sides of Eqs. (21a) and (21b), respectively. In diagrammatic form these sums are represented by linked but disconnected diagrams. Let us notice that for $n > 6$, $\langle(n)|H_N|e^{T_2}\Phi\rangle_C = 0$. Therefore, the equations representing projections onto higher-than-hexa-excited configurations can be expressed in terms of Eqs. (21a–f). Thus Eqs. (21a–f) represent all the linearly independent equations that arise when projecting Eq. (13) onto configurations spanning $\mathscr{F}_N$, Eq. (17). Note that when we deal with subsets of equations whose cardinality exceeds the number of unknown amplitudes, i.e. with overdetermined systems, the result also depends on the equation type, Eq. (13) or (15), that we choose in the projection procedure.

The terms on the left-hand side of Eqs. (21a–f) can be similarly characterized by the PT order as was done in Table 1 for Eqs. (18a–f). A glance at Eqs. (21c–f) reveals that the disconnected terms are of lower order in PT than the connected ones. Consequently, the projections on configurations of a given excitation order involve terms of a lower PT order than was the case for Eq. (15).

Consider, finally, the projections of Eqs. (13) and (15) with $T = T_2$ onto the mono-excited configurations, as given by the identical Eqs. (18a) and (21a). When employing HF spin orbitals, these can be cast into a form given by Eq. (19a). Notice that this equation differs from the standard CCD Eq. (18b) in several important points. First, it is linear in T_2. Second, it contains neither the absolute term nor the diagonal terms involving the energy denominators. Thus, Eq. (19a) cannot be used as a recursion equation to generate MBPT expansion for the t-amplitudes, as is the case for standard CCD equations (cf., e.g., [35]).

4. Example: L–CCD equations

As already alluded to above, the most meaningful exploitation of nonstandard CC equations, such as MM–CCD Eqs. (18), can be achieved by satisfying them in the least squares sense. Since this is computationally rather demanding for non-linear systems, we have decided to illustrate the above considerations on the linear version of the CCD (L–CCD) equations. For this purpose we have chosen two well studied, yet simple, systems, which involve a highly quasi-degenerate ground state reference, so that the L–CCD procedure suffers a singular behavior and thus completely breaks down once the quasi-degeneracy effects become significant and the intruder doubly excited states have lower energy than the restricted HF (RHF) reference. The first example involves the so-called H4 model [19, 39], consisting of two interacting, slightly stretched, H_2 molecules in a trapezoidal geometry, and the second one the cyclic polyene model, C_NH_N, with $N = 2n = 4v + 2$, $v = 1, 2, \ldots$, [40, 41].

4.1. *H4 model* [19, 39]

This model was examined in a considerable detail in our studies of the impact of quasi-degeneracy on various CCD approximations [19], and was subsequently the subject of several papers [39] exploring this problem for perturbative approaches. Since the size of the basis set used does not have any effect on the singular behavior [39f], we employ the simplest minimum basis set model as in Ref. [19].

The trapezoidal arrangement of the four hydrogen atoms, constituting the H4 model [19], is fully specified by a single parameter α once the internuclear separation between nearest neighboring atoms is fixed (at 2 a.u., see also Fig. 2 of [19]). For α approaching zero, the exact wavefunction involves strong quasi-degeneracy of the reference configuration $|\Phi\rangle$, while for $\alpha = 0.5$ (corresponding to the linear arrangement) these effects are removed and all the CCD approaches provide an excellent approximation. Another remarkable feature of this simple model is the fact that the linear approximation (L–CCD) breaks down completely in the strongly degenerate region, which is reflected by the presence of a singularity in the correlation energy as a function of α.

The four SCF MO's of this simple model are labeled according to their increasing orbital energies. The FCI wavefunction involves only two monoexcited $\left(\left|\begin{matrix}3\\1\end{matrix}\right\rangle, \left|\begin{matrix}4\\2\end{matrix}\right\rangle\right)$, six biexcited $\left(\left|\begin{matrix}33\\22\end{matrix}\right\rangle, \left|\begin{matrix}44\\22\end{matrix}\right\rangle, \left|\begin{matrix}33\\11\end{matrix}\right\rangle, \left|\begin{matrix}44\\11\end{matrix}\right\rangle, \left|\begin{matrix}34\\12\end{matrix}\right\rangle_s, \left|\begin{matrix}34\\12\end{matrix}\right\rangle_t\right)$, two triexcited (particle-hole conjugates of monoexcited), and one tetraexcited $\left(\left|\begin{matrix}3344\\1122\end{matrix}\right\rangle\right)$ orbital configurations [19]. Hence, after eliminating spin variables, Eqs. (18b) or (21b) are reduced to a system of six equations, defined by the above-mentioned biexcited orbital configurations onto which the Schrödinger equation is projected.

In the MM approach to the L–CCD scheme (MM–LCCD approach), we also have to consider two equations obtained by the projection onto the singly excited configurations and two more equations obtained by projection onto the triply excited configurations. Here we shall only examine the impact of the equations projected onto the monoexcited states, Eq. (19a). A version of the MM–LCCD approach, which involves equations projected onto the triply excited configurations, will be studied in the next example.

We require that the t_2-amplitudes are such that the set consisting of six standard L–CCD equations and two equations projected onto singly excited states is satisfied as best as possible in the least squares sense, i.e., we minimize the expression

$$R \equiv p \sum_{\substack{a_1a_2\\ r_1r_2}} \left| \left\langle \begin{matrix} r_1r_2 \\ a_1a_2 \end{matrix} \right| H_N \left| (1+T_2)\Phi \right\rangle \right|^2 + q \sum_{a,r} \left| \left\langle \begin{matrix} r \\ a \end{matrix} \right| H_N \left| (1+T_2)\Phi \right\rangle \right|^2, \tag{22}$$

where p and q are weighting factors, $p+q=1$. These weighting factors are included in order to take into account the above-mentioned fact that the two sums involve terms of different order in the PT sense and that the number of equations in various subsets corresponding to different excitation order projections may greatly differ. The condition that minimizes R, Eq. (22), results in a set of linear equations for the t_2-amplitudes (see Sect. 4.2 for more detail).

The results of our calculations of the correlation energy are presented in Table 2, where they are compared with standard L–CCD and CCD results as well as with the exact FCI values. The L–CCD energy has a singularity for $\alpha \approx 0.018$. We can see from Table 2 that for all the values of the parameter p considered, the correlation energy shows no singularity whatsoever, which indicates that taking into account the additional nonstandard equations decreases the impact of the singularity of the coefficient matrix of the L–CCD approach (cf. [21]). It is also apparent from the table that irrespective of the p-value, the results of the present method are in better agreement with the FCI energies than the standard ones. This agreement improves spectacularly when proceeding to very small p-values, i.e., when the ratio q/p in Eq. (22) becomes very large. This behavior seems to be a consequence of the fact that the terms in the second sum, representing the fourth-order quantities, are much smaller than the terms in the first sum that contain second-order contributions. A comparison of the results for $p = 10^{-6}$ and $p = 10^{-8}$ indicates that a further reduction of p will not result in any significant change of the correlation energy. Thus, an inclusion of nonstandard equations obtained by projections onto the monoexcited configurations has a similar effect on the removal of a singular behavior of the L–CCD method as has the inclusion of the non-linear terms (for a review of results obtained at various stages of inclusion of such terms, see [19]).

As mentioned earlier, another possibility of employing the additional CC equations that are generated by nonstandard projections is to use them in lieu of standard ones, while preserving the total number of equations (given by the number of unknown t-amplitudes). In Table 2 we present the results for three such selections. In the first two, the equation obtained by projecting onto the orbital configuration $\left|\begin{smallmatrix}34\\12\end{smallmatrix}\right\rangle_t$ is replaced, in turn, by the projections onto $\left|\begin{smallmatrix}3\\1\end{smallmatrix}\right\rangle$ and onto $\left|\begin{smallmatrix}4\\2\end{smallmatrix}\right\rangle$. The set of equations in the third selection is obtained by replacing the projections onto $\left|\begin{smallmatrix}44\\22\end{smallmatrix}\right\rangle$ and $\left|\begin{smallmatrix}34\\12\end{smallmatrix}\right\rangle_t$ by the projections onto $\left|\begin{smallmatrix}3\\1\end{smallmatrix}\right\rangle$ and $\left|\begin{smallmatrix}4\\2\end{smallmatrix}\right\rangle$. We see from the table that the energies so obtained are much better than those obtained with the traditional L–CCD approach. The improvement is particularly evident in the region of strong quasi-degeneracy. This is easily understood if we realize that we have replaced the equations that are primarily responsible for the singularity of the L–CCD coefficient matrix by equations obtained through nonstandard projections.

4.2. *Cyclic polyene model* [40, 41]

Let us next investigate the cyclic polyene model [40, 41] $C_N H_N$, $N = 2n = 4\nu + 2$, $\nu = 1, 2, \ldots$, with non-degenerate ground state, as described by the Pariser–Parr–Pople (PPP) semiempirical model Hamiltonian [42]. This system represents a very useful model of quasi-one-dimensional metallic-like polymers and has been extensively studied in connection with dimerization of polyacetylene [43], which is crucial for understanding of the electrical conductivity as well as of various magnetic and optical properties in these potentially very useful materials [44]. Simultaneously, this model represents an extremely challenging problem, since its RHF reference state becomes highly quasi-degenerate when $N \to \infty$ (in practice $N \sim 20$), so that even standard CCD approach breaks down [41d,e]. We note that for highly symmetric, undistorted models with the nuclear framework forming a regular N-gon, the MO's are completely determined by the symmetry (representing simultaneously HF and Brueckner orbitals). Thus, the monoexcited cluster component T_1 exactly vanishes in this case and, likewise, Eqs. (18a) or (19a) are automatically satisfied, so that we can ignore monoexcitations altogether. Since the complete set of the MM–LCCD equations for cyclic polyenes consists now of only the equations projected onto doubly and triply excited states, we minimize the following expression [see Eqs. (18b) and (18c); cf. with Eq. (22)]:

$$R \equiv p \sum_{(2)} |\langle(2)|V_N + H_N T_2|\Phi\rangle|^2 + q \sum_{(3)} |\langle(3)|V_N T_2|\Phi\rangle|^2, \qquad (23)$$

Table 2. Correlation energies for the H4 model [19] obtained by means of the nonstandard MM approach to the L–CCD and comparison with results of standard L–CCD, CCD and FCI approaches (in mH, all signs reversed)

	Least Squares			Replacements[a]					
α	$p = 0.5$	$p = 10^{-6}$	$p = 10^{-8}$	$D_6 \to S_1$	$D_6 \to S_2$	$D_2, D_6 \to S_1, S_2$	L–CCD[b]	CCD[b]	FCI[b]
0.500	55.849	51.586	51.586	51.932	48.710	55.451	56.260	53.572	53.690
0.200	60.390	59.164	59.153	57.501	58.961	55.982	60.553	57.233	57.260
0.100	70.891	68.901	68.901	68.197	71.818	63.990	71.017	65.318	65.321
0.050	89.762	79.855	79.855	79.826	83.148	75.534	91.829	76.635	76.429
0.020	135.133	86.127	86.125	91.499	93.142	89.483	320.410	93.034	92.148
0.015	41.358	86.568	86.565	94.125	95.114	92.950	−517.543	97.900	96.711
0.005	−5.899	86.455	86.440	100.388	99.170	101.708	−8.129	111.355	109.196

[a] S_1, S_2, D_2, and D_6 denote projections onto the orbital configurations $\left|\begin{matrix}3\\1\end{matrix}\right\rangle$, $\left|\begin{matrix}4\\2\end{matrix}\right\rangle$, $\left|\begin{matrix}44\\22\end{matrix}\right\rangle$, and $\left|\begin{matrix}34\\12\end{matrix}\right\rangle_t$, respectively

[b] From Ref. [19]

where again $p + q = 1$. We dropped the subscript C in Eq. (23), since there is no contribution from the disconnected terms in the matrix elements entering R [cf. Eq. (22)]. Rewriting this expression with the help of projection operators $Q^{(j)}$,

$$Q^{(j)} = \sum_{(j)} |(j)\rangle\langle(j)|, \qquad j = 2, 3, \tag{24}$$

we have:

$$\begin{aligned} R = p &\left[\langle \Phi | V_N Q^{(2)}(V_N + H_N T_2) | \Phi \rangle + \sum_j t_j^* \langle \Phi_j | H_N Q^{(2)}(V_N + H_N T_2) | \Phi \rangle \right] \\ &+ q \sum_j t_j^* \langle \Phi_j | V_N Q^{(3)} V_N T_2 | \Phi \rangle, \end{aligned} \tag{25}$$

where, for simplicity, we write the pair cluster component as follows:

$$T_2 = \sum_i t_i C_2(i), \qquad T_2^\dagger = \sum_i t_i^* C_2(i)^\dagger, \tag{26}$$

the sum extending over all biexcited configurations $\Phi_i = C_2(i)\Phi$. Thus, the necessary condition for the minimum of R, $\partial R/\partial t_i^* = \partial R/\partial t_i = 0$, results in a linear system of equations for the t_2-amplitudes, namely:

$$\begin{aligned} &p\left(\sum_k \langle \Phi_i | H_N | \Phi_k \rangle \langle \Phi_k | V_N | \Phi \rangle + \sum_{k,j} \langle \Phi_i | H_N | \Phi_k \rangle \langle \Phi_k | H_N | \Phi_j \rangle t_j \right) \\ &\qquad + q \sum_j \langle \Phi_i | V_N Q^{(3)} V_N | \Phi_j \rangle t_j = 0, \end{aligned} \tag{27}$$

and its complex conjugate.

Introducing the standard notation for the elements of $\boldsymbol{a}$, $\boldsymbol{b}$ and $\bar{\boldsymbol{W}}$ matrices:

$$\begin{aligned} a_i &= \langle \Phi_i | H_N | \Phi \rangle = \langle \Phi_i | V_N | \Phi \rangle, \\ b_{ij} &= \langle \Phi_i | H_N | \Phi_j \rangle, \\ \bar{W}_{ij}^{(3)} &= \langle \Phi_i | V_N Q^{(3)} V_N | \Phi_j \rangle, \end{aligned} \tag{28}$$

we can write the system (27) as follows:

$$p\boldsymbol{b}(\boldsymbol{a} + \boldsymbol{b}\boldsymbol{t}) + q\bar{\boldsymbol{W}}^{(3)}\boldsymbol{t} = 0, \tag{29}$$

where $\boldsymbol{t}$ is the column matrix of pair cluster amplitudes, $\boldsymbol{t} = (t_1 t_2 \ldots)^T$. Finally, we can write the relevant MM–LCCD equations in the form:

$$\left(\boldsymbol{b}^2 + \frac{1-p}{p} \bar{\boldsymbol{W}}^{(3)} \right) \boldsymbol{t} + \boldsymbol{b}\boldsymbol{a} = 0, \tag{30}$$

so that for $p = 1$ we recover standard L–CCD equations. The correlation energy is given by the standard expression:

$$\Delta E = \boldsymbol{a}^\dagger \boldsymbol{t}. \tag{31}$$

We also note that the term involving triple excitations, $\bar{\boldsymbol{W}}^{(3)}$, has a similar structure (except for the denominators) as the $\boldsymbol{W}^{(3)}$ term occurring in the recently considered CCDT-1 and ACPTQ approaches [41f, 45] as well as in the optimized inner projection approach [45–47]. Thus, we were able to use very much the same code as in these studies [41f, 47].

We have examined the MM–LCCD solutions for cyclic polyenes with $\nu = 1$–5 in both PPP and Hubbard Hamiltonian descriptions, using the same parametrization as in our earlier studies [41]. The whole range of the coupling constant, as well as of the parameter $p = 1 - q$, was investigated in each case. We recall [41d–f] that the standard L–CCD approach suffers a highly singular behavior in the intermediately and strongly correlated regions, the number of singularities rapidly increasing with increasing N and extending to higher and higher $|\beta|$ values (β designates the resonance or hopping integral, whose reciprocal value can be regarded as a coupling constant; the physical value of β is about -2.5 eV, $\beta = 0$ represents the strongly correlated limit, while $\beta \sim -5$ eV corresponds already to a weakly correlated regime; see [41d–f] for details).

Here we should emphasize that even the full CCD approach encounters serious difficulties when applied to cyclic polyene models. In the strongly correlated region of $N = 6$ and 10 polyenes, the resulting correlation energies are very poor, while for $N \geqslant 14$ there exists a critical resonance integral value β_c, beyond which the solutions of the CCD equations become complex [41d,e]. The critical value β_c shifts towards the weakly coupled region with increasing polyene size, so that already for the $N = 26$ PPP model, the solutions of the standard CCD equations are not available even for the physical parametrization. Our studies [41d,f] indicate that the critical resonance integral value β_c is a branch point in the correlation energy regarded as a function of β, and that the poor performance of the CCD approach is a result of the neglect of connected quadruply excited clusters [41b,d,e,g].

A typical behavior of the MM–LCCD energies in the strongly correlated regime is illustrated in Fig. 2 for the $C_{10}H_{10}$ ring, in which case the exact result is available for both PPP [41b] and Hubbard [48] Hamiltonian descriptions. This figure clearly indicates that already for $N = 10$ the CCD approach essentially breaks down in the highly correlated region, even though the solution still exists. The MM–LCCD energies, already for very small $q = 1 - p$ values, show only the remnants of the singular behavior and get gradually "smoothed out" with decreasing p. It is remarkable that even for very small p values (10^{-3}–10^{-10}) the MM–LCCD energies show a more or less correct β dependence, although shifted towards smaller absolute energy values, as may be seen from Fig. 3 showing the β dependence of the correlation energy for the $N = 22$ ring in weakly and intermediately coupled regions. Indeed, MM–LCCD can provide good correlation energies for $|\beta| \geqslant 1.5$ eV ($N = 6$–14) and $|\beta| \geqslant 2$ eV ($N = 18$ and 22). For the Hubbard models, the MM–LCCD energies are quite satisfactory up to $\beta = -1$ eV. The nonsingular behavior of the MM–LCCD energies in the whole range of the coupling constant, particularly for the Hubbard Hamiltonian models, and the fact that it recovers a nonnegligible part of the correlation energy well beyond the first singularity of the standard L–CCD approach, are truly remarkable in view of the simplicity of the procedure and the fact that no account of important quadruple excitations is taken.

Examining the results for $6 \leqslant N \leqslant 22$ and different p values, we have noticed that with increasing N the optimal p values tend to 1. As already indicated above, this is most likely related to the fact that the number of triples n_T grows much faster than the corresponding number of pair clusters n_D. The optimal p value seems to correlate quite well with the ratio $n_T/(n_D + n_T)$ and changes from about 0.3–0.4 for $N = 6$ to about 0.9 for $N = 22$. These observations are only of a very preliminary character and an investigation of a possibility to estimate independently the p value would be most desirable.

It is an interesting observation that for sufficiently small values of p, the MM–LCCD correlation energies represent upper bounds to their exact values

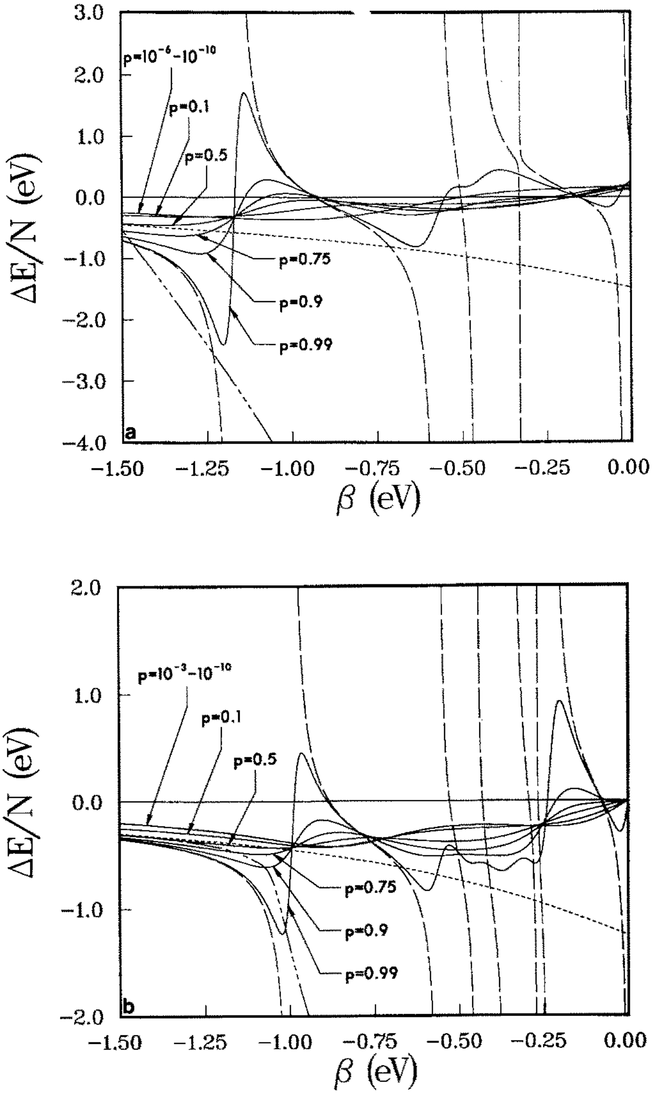

Fig. 2. MM-LCCD correlation energies per electron, $\Delta E/N$, (in eV) for the $N = 10$ PPP (*a*) and Hubbard (*b*) cyclic polyene models in the strongly correlated region for various values of the weighting factor p (*solid lines*). Resonance integral dependence of the exact (full CI) [41b] (*short-dashed line*), L-CCD (*long-dashed line*) and full CCD (*chain-dashed line*) correlation energies per electron is presented for a comparison

(cf. Figs. 2 and 3). For $N \geqslant 10$, this is true in the entire region of the coupling constant. This property of the MM-LCCD approach should be compared with the well-known property of the standard L-CCD approach (or MM-LCCD approach with $p = 1$), which usually provides a lower bound (see, e.g., [2]; cf. Fig. 3).

5. Structure and definiteness of the CC wavefunction

We have seen that, within the framework of the MM approach, we can generate various sets of CC-type equations for cluster amplitudes, depending on the way

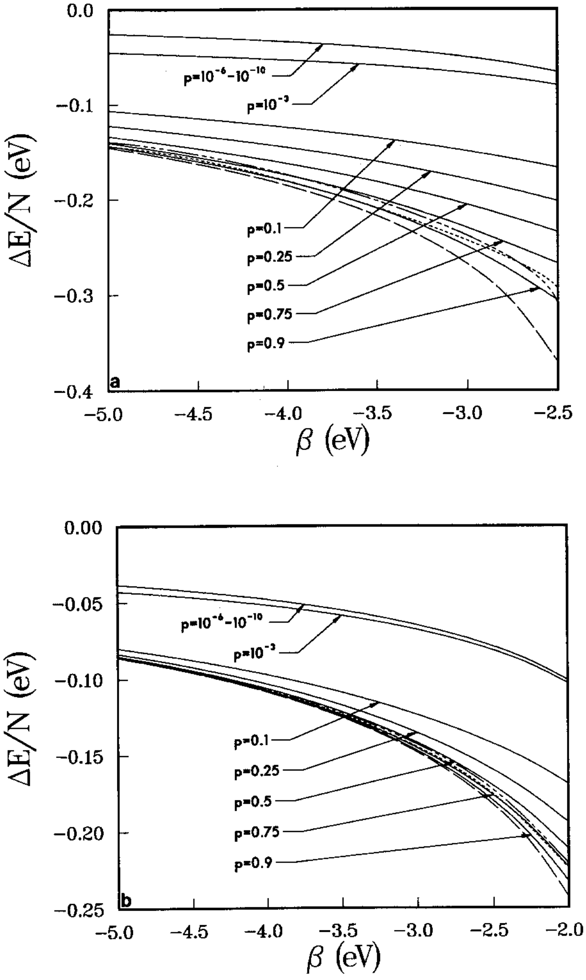

Fig. 3. MM–LCCD correlation energies per electron, $\Delta E/N$, (in eV) for the $N=22$ PPP (*a*) and Hubbard (*b*) cyclic polyenes in the region of nonsingular behavior of the standard L–CCD and full CCD approaches for various values of the weighting factor p (solid lines). Exact data for the $N=22$ PPP model are not available. Thus, the short-dashed line in (*a*) represents the correlation energy per electron as obtained with the ACPQ + T(ACPQ) method [41h], which provides us with the best available estimates for the ground-state correlation energies of cyclic polyenes with large N's. Short-dashed line in (*b*) represents the exact correlation energy per electron as obtained [48] by solving the Lieb and Wu equations [49]. Resonance integral dependence of the L–CCD (long-dashed line) and full CCD (chain-dashed line) correlation energies per electron is presented for a comparison. The large curvature of the curve representing the full CCD results for the PPP model in the region of spectroscopic β value (-2.5 eV) reflects the presence of the first-order algebraic branch point at $\beta_c=-2.34$ eV [41d,f] (cf. the text for details)

of projecting the Schrödinger equation. Hence, we obtain different wavefunctions of the form $|e^T\Phi\rangle$, approximating the same exact wavefunction $|\Psi\rangle$. Clearly, in order to determine uniquely the cluster amplitudes and thus the cluster operator T within the general context of the MM approach, we have to specify not only the coordinate space used, but also our choice of the projection space.

In this context it is useful to realize that in fact we seldom fully exploit the highly excited states that are automatically involved in the CC wavefunction. Let us illustrate this point on the CCD approach where

$$|\Psi_{\mathrm{CCD}}\rangle = e^{T_2}|\Phi\rangle, \tag{32a}$$

or, when $N=2n$,

$$|\Psi_{\mathrm{CCD}}\rangle = e^{T_2}|\Phi\rangle = \left(1 + T_2 + \frac{1}{2!}T_2^2 + \cdots + \frac{1}{n!}T_2^n\right)|\Phi\rangle. \tag{32b}$$

Now, when using the standard approach, the cluster components of T_2 are determined by equivalent systems of Eqs. (14b) and (16b). Clearly, only the first three terms in the expansion on the rightmost side of Eq. (32b) give nonzero contributions to the standard Eqs. (14b) or (16b). Thus, strictly speaking, the following wavefunction:

$$|\Psi'_{\mathrm{CCD}}\rangle = (1 + T_2 + \tfrac{1}{2}T_2^2 + \alpha_3 T_2^3 + \cdots + \alpha_m T_2^m)|\Phi\rangle, \tag{33}$$

with arbitrary α_i ($i = 3, \ldots, m$), will lead to the same CCD equations as the true CCD wavefunction, Eq. (32a). One might thus think that in fact the CCD wavefunction is not unique, since we can obtain the same CCD energy, given by Eqs. (14a) or (16a), and the same t_2-amplitudes given by Eqs. (14b) or (16b), for an arbitrary choice of α_i, $i = 3, \ldots, m$, in Eq. (33). However, we know from Hubbard's work that the exact wavefunction, which will possess the correct size-extensive property, must have the form given by Eq. (6). Thus, truncating T to T_2, the correctly behaving wavefunction to this approximation must have the form (32a). Now, in order to determine this wavefunction, we only have to specify the T_2 cluster amplitudes, whose number equals the number of linearly independent biexcited configurations M_2. Consequently, these can be determined by projecting onto the space of the same dimension. The most natural choice for this projection space is clearly the standard one. However, nonstandard equations might prove useful, particularly when the standard choice is plagued with singularities, as may be the case in quasi-degenerate situations. This was demonstrated in the preceding section on the L–CCD case for the H4 and C_NH_N models.

It is also only in this sense that the CCD, or any other CC, approach accounts for the disconnected hexa-, octa-, etc. excited cluster components. Indeed, these terms only occur explicitly in the general MM approach to CCD, as discussed above, when the full set of MM equations, Eqs. (18a–f) or (21a–f), involves projections onto mono-, bi-, . . . , hexa-excited configurations and contains terms up to the fourth power in T_2. However, as stated already, any subset of M_2 independent equations will determine a set of M_2 t_2-amplitudes. Clearly, the standard set represents the most meaningful choice from the viewpoint of either the MBPT or CI, as discussed above. However, when this set is ill-conditioned or even singular, other choices might be preferred. A more detailed investigation of these options would be clearly desirable.

6. Conclusions

We attempted to provide a novel insight into the CC theory by interpreting its basic equations from the viewpoint of the method of moments. Within this approach, in addition to the usual set of equations for cluster amplitudes that result from the so-called standard projections (projections onto excited configurations that occur in the cluster operator considered) we also obtain equations resulting from projections onto the nonstandard configurations. To understand the significance of the latter, we have derived the full set of MM equations for the CCD case. Within this set, the standard equations are characterized by the fact that they involve terms contributing to the correlation energy in the lowest order of PT. However, among the equations associated with nonstandard projections there are such that contain terms of the same order of PT as certain terms of standard equations. Consideration of these nonstandard equations may be of interest in practical applications, as we demonstrated for the L–CCD approach applied to two simple models involving quasi-degeneracy.

Acknowledgements. A continued support by NSERC (JP) is gratefully acknowledged, as well as partial support by the Polish Academy of Sciences (KJ) within the project C.P.B.P.-01.12. The authors wish to thank Professors Rodney Bartlett and Bogumił Jeziorski for valuable comments and suggestions. We (KJ and JP) are also very much obliged to Professor Bartlett for enabling us to take part in the most stimulating "Workshop on Coupled-Cluster Theory at the Interface of Atomic Physics and Quantum Chemistry" at the Harvard Smithsonian Center for Astrophysics and to present the ideas contained in this paper. Two of the authors (KJ and PP) would also like to express their sincere thanks to their co-author, Professor J. Paldus, for the warm hospitality extended to them during their visit to the Department of Applied Mathematics at the University of Waterloo.

References

1. Bartlett R (1981) Annu Rev Phys Chem 32:359
2. Paldus J (1983) Coupled cluster approaches to many-electron correlation problem. In: Löwdin P-O, Pullman B (eds) New horizons of quantum chemistry. Reidel, Dordrecht, pp 31–60
3. Bartlett RJ, Dykstra CE, Paldus J (1984) Coupled cluster methods for molecular calculations. In: Dykstra CE (ed) Advanced theories and computational approaches to the electronic structure of molecules. Reidel, Dordrecht, pp 127–159
4. Bartlett RJ (1989) J Phys Chem 93:1697
5. Wilson S (ed) (1987) Methods in computational chemistry, vol 1, Electron correlation in atoms and molecules. Plenum, New York; see chapters by Jankowski K, pp 1–101, and by Urban M, Černušák I, Kellö V, Noga J, pp 117–239
6. Kaldor U (ed) (1989) Many-body methods in quantum chemistry, Lecture notes in chemistry, vol 52. Springer, Berlin (see sections on Coupled cluster methods and Quadratic configuration interaction, pp 125–232)
7. Jeziorski B, Monkhorst HJ (1981) Phys Rev A24: 1668; Lindgren I, Mukherjee D (1987) Phys Rep 151:93; Jeziorski B, Paldus J (1989) J Chem Phys 90:2714
8. Chiles RA, Dykstra CE (1981) J Chem Phys 74:4544
9. Purvis GD, Bartlett RJ (1982) J Chem Phys 76:1910; Noga J, Bartlett RJ (1987) ibid 86:7041; (1988) ibid 89:3401 (E)
10. Szalewicz K, Zabolitzky JG, Jeziorski B, Monkhorst HJ (1984) J Chem Phys 81:2723
11. Geertsen J, Oddershede J (1986) J Chem Phys 85:2112
12. Čárský P, Schaad LJ, Hess BA (1987) J Chem Phys 87:411
13. Scuseria GE, Scheiner AC, Lee TJ, Rice JE, Schaefer HF III (1987) J Chem Phys 86:2881; Scuseria GE, Schaefer HF III (1988) Chem Phys Lett 152:382
14. Pople JA, Head-Gordon M, Raghavachari K (1987) J Chem Phys 87:5968 (cf. also: idem (1989) ibid 90:4635 and Paldus J, Čížek J, Jeziorski B (1989) ibid 90:4356)
15. Kantorovich LV, Krylov VI (1958) Approximate methods of higher analysis. Interscience, New York, p 150
16. Szondy T (1963) Acta Phys Hung 17:303; Hedgyi MG, Mezei M, Szondy T (1969) Theor Chim Acta 15:273
17. Boys SF (1969) Proc Roy Soc (London) A309:195
18. Jankowski K (1976) Int J Quantum Chem 10:683; Jankowski K, Rutkowski A (1976) Theor Chim Acta 43:145; Jankowski K, Rutkowska D, Rutkowski A (1978) ibid 48:119
19. Jankowski K, Paldus J (1980) Int J Quantum Chem 18:1243
20. Adams BG, Jankowski K, Paldus J (1979) Chem Phys Lett 67:144; idem (1981) Phys Rev A24:2316, 2330
21. Paldus J, Wormer PES, Visser F, van der Avoird A (1982) J Chem Phys 76:2458
22. Coester F (1958) Nucl Phys 7:421; Coester F, Kümmel H (1960) Nucl Phys 17:477
23. Čížek J (1966) J Chem Phys 45:4256; idem (1969) Adv Chem Phys 14:35
24. Klahn B, Bingel WA (1977) Theor Chim Acta 44:9, 27; Bongers A (1977) Chem Phys Lett 49:393

25. Goldstone J (1957) Proc Roy Soc (London) A239:267
26. Hubbard J (1957) Proc Roy Soc (London) A240:539; idem (1958) ibid A243:336, A244:199
27. Mayer JE, Mayer MG (1940) Statistical mechanics. Wiley, New York, ch 13
28. Primas H (1965) Separability in many-electron systems. In: Sinanoğlu O (ed) Modern quantum chemistry, Istanbul lectures, Part II, Interactions. Academic Press, New York, pp 45–74
29. For details, see e.g.: Krasnosel'skii MA, Vainikko GM, Zabreiko PP, Rutitskii YaB, Stetsenko VYa (1972) Approximate solution to operator equations, ch 4. Wolters-Noordhoff Publishing, Groningen
30. Čížek J, Paldus J (1971) Int J Quantum Chem 5:359
31. Bartlett RJ, Purvis GD (1978) Int J Quantum Chem 14:561
32. Kümmel H, Lührmann KH, Zabolitzky JG (1978) Phys Rep C36:1
33. Paldus J, Čížek J, Jeziorski B (1989) J Chem Phys 90:4356
34. Arponen J (1983) Ann Phys 151:311; Arponen JS, Bishop RF, Pajanne E (1987) Phys Rev A 36:2519; Robinson NI, Bishop RF, Arponen J (1989) ibid 40:4256
35. Paldus J (1977) J Chem Phys 67:303
36. Paldus J, Čížek J (1975) Adv Quantum Chem 9:105
37. Handy NC, Pople JA, Head-Gordon M, Raghavachari K, Trucks GW (1989) Chem Phys Lett 164:185; Raghavachari K, Pople JA, Replogle ES, Head-Gordon M, Handy NC (1990) ibid 167:115
38. Chiles RA, Dykstra CE (1981) J Chem Phys 74:4544
39. (a) Wilson S, Jankowski K, Paldus J (1983) Int J Quantum Chem 23:1781; (b) Pulay P (1983) Int J Quantum Chem S17:257; (c) Kaldor U (1985) Int J Quantum Chem 28:103; (d) Wilson S, Jankowski K, Paldus J (1985) ibid 28:525; (e) Iijima N, Saika A (1985) ibid 27:481; (f) Paldus J, Wormer PES, Benard M (1988) Coll Czech Chem Commun 53:1919; (g) Zarrabian S, Paldus J (1990) Int J Quantum Chem 38:761
40. Pauncz R, de Heer J, Löwdin P-O (1962) J Chem Phys 36:2247, 2257; de Heer J, Pauncz R (1960) J Mol Spectr 5:326; Pauncz R (1967) Alternant molecular orbital method. Saunders, Philadelphia
41. (a) Paldus J, Čížek J (1970) Phys Rev A2:2268; (b) Paldus J, Boyle MJ (1982) Int J Quantum Chem 22:1281; (c) Takahashi M, Paldus J, Čížek J (1983) ibid 24:707; (d) Paldus J, Takahashi M, Cho RWH (1984) Phys Rev B30:4267; (e) Takahashi M, Paldus J (1985) ibid 31:5121; (f) Piecuch P, Zarrabian S, Paldus J, Čížek J (1990) ibid 42:3351; (g) Paldus J, Takahashi M, Cho BWH (1984) Int J Quantum Chem S18:237; (h) Paldus J, Piecuch P (1991) Int J Quantum Chem XX:XXX
42. Parr RG (1963) The quantum theory of molecular electronic structure. Benjamin, New York
43. Paldus J, Chin E (1983) Int J Quantum Chem 24:373; Takahashi M, Paldus J (1985) ibid 28:459 and references therein
44. See, for example, Baeriswyl D, Campbell DK, Mazumdar S (1990) An overview of the theory of π-conjugated polymers. In: Kiess H (ed) Conducting polymers. Springer-Verlag, Berlin
45. Piecuch P, Paldus J (1990) Theor Chim Acta 78:65; Čížek J, Vinette F, Paldus J (1990) Int J Quantum Chem 38:831
46. Čížek J, Vinette F, Paldus J (1989) Diagrammatic approach to the calculation of the lower bounds using optimized inner projection technique. Application to the cyclic polyene model. In: Kaldor U (ed) Many-body methods in quantum chemistry. Springer-Verlag, Berlin, pp 23–42
47. Piecuch P, Zarrabian S, Paldus J, Čížek J (1990) Phys Rev A 42:5155
48. Hashimoto K, Čížek J, Paldus J (1988) Int J Quantum Chem 34:407
49. Lieb EH, Wu FY (1968) Phys Rev Lett 20:1445
50. Mukherjee D (1981) Chem Phys Lett 79:559